NASA Technical Memorandum 83755

The Effects of Lithium Counterdoping on Radiation Damage and Annealing in n^+p Silicon Solar Cells

I. Weinberg, H. W. Brandhorst, Jr., S. Mehta,
and C. K. Swartz
Lewis Research Center
Cleveland, Ohio

Prepared for the
Fourth European Symposium on Photovoltaic Generators in Space
Cannes, France, September 18–20, 1984

NASA

THE EFFECTS OF LITHIUM COUNTERDOPING ON RADIATION DAMAGE AND ANNEALING IN n^+p SILICON SOLAR CELLS

I. Weinberg, H. W. Brandhorst, Jr., S. Mehta* and C. K. Swartz

National Aeronautics and Space Administration
Lewis Research Center
Cleveland, Ohio 44135

E-2243

ABSTRACT

Boron-doped silicon solar cells were counterdoped with lithium and the resultant n^+p cells irradiated by 1 MeV electrons. It was found that the lithium counterdoped cells exhibited significantly increased radiation resistance with considerable annealing occurring at 100° C. DLTS studies indicate that the annealing behavior is controlled by a single defect at $E_V + 0.43$ eV. It is concluded that the increased radiation resistance of the counterdoped cells is due primarily to the interaction of lithium with oxygen, single vacancies and divacancies. It is speculated that the lithium-oxygen interaction is the most effective in contributing to the increased radiation resistance.

Keywords: Radiation damage; Lithium counterdoped silicon solar cells; Defects

INTRODUCTION

In the past, extensive studies have been conducted on p^+n silicon solar cells in which lithium was used as the n-dopant (Refs. 1-2). Although some advantage, under 1 MeV electron irradiation was found at elevated temperatures, in general, the cells emanating from this terminated program were found to exhibit the same tolerance to 1 MeV electron irradiation as conventional n^+p silicon solar cells. We report here results on lithium counterdoped n^+p silicon solar cells in which lithium is introduced into the boron doped p-region in small enough quantities so that, despite the compensating effects of lithium, the cell base remains p-type. This procedure was followed in order to exploit the increased radiation resistance of p-type over n-type silicon (Ref. 3). The present work is an extension of our earlier work on electron-irradiated low resistivity, lithium counterdoped n^+p silicon cells (Ref. 4). It differs from our earlier work in the use of higher resistivity silicon and the use of ion implantation in introducing the lithium. We have, in addition, investigated the radiation induced deep level defects by Deep Level Transient Spectroscopy (DLTS).

*Cleveland State University, Cleveland, Ohio and NASA Intern.

EXPERIMENTAL

The cells were fabricated from 1 ohm-cm boron-doped float zone silicon. All cells were 2 by 2 cm, 250 μm thick with no antireflection coating. The cell's n^+ region was formed by phosphorus ion implantation while the lithium was introduced by implantation of lithium ions into the front and back of the cell. Electron beam annealing was used to selectively anneal the n^+ region after ion-implantation (Ref. 6). Lithium concentrations were determined by four point resistivity measurements at the back surface and C-V measurements at the junction. For comparison purposes, n^+p control cells were fabricated by phosphorus ion implantation into the boron doped 1 ohm-cm float zone silicon. Cell characteristics are shown in Table I. After fabrication, the cells were irradiated by 1 MeV electrons and solar cell parameters determined using an AMO xenon-arc solar simulator. DLTS measurements were performed on small area portions of the cells (0.01 to 0.03 cm^2) using a 30 MHz capacitance bridge and boxcar averager (Ref. 5). To prevent extraneous annealing, the cells were immersed in liquid nitrogen between irradiations, measurements and isochronal anneals.

RESULTS

From Table I it is seen that the pre-irradiation power output levels are less for the lithium counterdoped cells. However, with irradiation, the effects of lithium are such that the output power of the counterdoped cells exceeds that of the control cells (Fig. 1). This can also be seen from Fig. 2 which shows normalized maximum power for all cells after completion of the irradiations. Parenthetically, it is noted that, prior to irradiation, the open circuit voltages of the counterdoped cells are less than that of the control cell. On the other hand, for all but one of the counterdoped cells, the pre-irradiation short circuit current is greater than that of the control cell. A further discussion of the pre-irradiation behavior of these cells is found in Appendix A.

The effects of 20 min isochronal annealing are shown in Fig. 3 where it is seen that significant cell recovery occurs for $T \leq 100^{\circ}$ C. It is noted here that, at these temperatures, thermal degradation of space solar array components is minimal. Hence the present cells with further optimization could be candidates for components of an annealable array.

The dependence of power loss on lithium gradients is shown in Fig. 4. In all cases, the gradients are such that the lithium concentration is greatest at the rear of the cell. Previous data and calculations on lithium gradients for p^+n cells indicate a correlation between cell performance and gradient (Refs. 7-8). However this is not the case for the present cells.

A DLTS spectrum, showing both minority and majority carrier recombination centers is shown in Fig. 5 for the lithium counterdoped cells. From the figure, four deep level defects are detected with energy levels as shown. One result of lithium addition is the formation of new defects. This can be seen from Table II where the energy levels and capture cross sections of the counterdoped cells can be compared to those of the boron doped control cells. Isochronal annealing data for the defects in the counterdoped cells are shown in Fig. 6. Comparison with Fig. 3 shows a correlation between the isochronal annealing behavior of the defect at $E_V + 0.43$ eV and recovery of short circuit current.

DISCUSSION

Cell Performance After Irradiation

The significant improvement over the control cells, after irradiation, observed in the present case is much greater than the slight improvement previously noted in our earlier work on lithium counterdoped n^+p cells (Ref. 4). These latter cells were processed from 0.35 ohm-cm float zone and Czochralski grown silicon the results indicating that float zone was preferable and that positive or zero lithium gradients were preferable to negative lithium gradients. Our present use of float zone silicon and the avoidance of negative lithium gradients follows the recommendations emanating from our earlier work (Ref. 4). The present, comparatively much greater improvement in radiation resistance could possibly be due to the use of higher resistivity silicon and/or the different processing technique used. With respect to processing, we recall that previously the lithium was applied as a paste to the cell's back surface followed by heating to drive in the lithium (Ref. 4). Concerning the absence of a definite correlation between gradient and performance, we note that the gradients found in the present n^+p cells are at least an order of magnitude lower than those cited for the p^+n cells where dependence of cell output on lithium gradient was previously reported (Refs. 7-8).

Annealing

Comparison of Figs. 3 and 6 shows a strong correlation between the annealing behavior of the defect at $E_V + 0.43$ eV and cell performance. A similar correlation is observed for diffusion length in Fig. 7. These data indicate that the $E_V + 0.43$ defect is dominant in controlling the annealing behavior of the present counterdoped cells.

Interaction with Lithium

Little is known concerning the composition of the defects which correspond to the energy levels and capture cross sections of the deep level defects detected by DLTS in the counterdoped cell. However, much more is known concerning the defects in the boron doped control cells. In addition, there is a background of information, obtained by other techniques, on the composition of defects in lithium-doped silicon. For example, it is known that lithium combines with divacancies (Ref. 9), oxygen (Ref. 10), and substitutional boron (Ref. 10) in silicon. This information can be used to speculate on the interactions involving lithium which lead to the increased radiation resistance we observe in the present counterdoped cells. Therefore in the remainder of this discussion we consider the defects in the boron doped cells and the possible interactions with lithium which could lead to the changes observed in the counterdoped cells.

Defect at $E_C - 0.27$ eV

This defect has been tentatively identified as a complex of interstitial oxygen and interstitial boron (Ref. 11). A later investigation tends to confirm the identification as a boron-oxygen complex (Ref. 11). Since the complex is positively charged (Ref. 11), we assume no interaction with lithium which takes the form Li^+ in silicon. However lithium is known to combine with interstitial oxygen and substitutional boron in silicon (Ref. 10). Of these latter two interactions it is more likely that lithium in combining with interstitial oxygen would tend to inhibit formation of this defect.

Defect at $E_V + 0.23$ eV

This defect has been identified as the divacancy (Refs. 11, 13). It has also been established that lithium forms complexes with divacancies (Ref. 9). Hence it is concluded that this defect is altered on counterdoping predominantly by the complexing of lithium with divacancies.

Defect at $E_V + 0.33$ eV

This defect has been alternately identified, from DLTS data, as a vacancy-oxygen-carbon complex (Ref. 11) or as a carbon interstitial-carbon substitutional pair (Ref. 14). In both cases, the DLTS peak anneals at $T \sim 400^{\circ}$ C (Refs. 11,14). It is well to note that the DLTS data, by itself, does not suffice to identify the atomic constituents of a defect. Other data, for example EPR, is usually required to identify a specific complex. In this connection, it is significant to note that the EPR spectrum associated with the carbon-carbon pair anneals at $T \sim 300^{\circ}$ C (Ref. 15) while the EPR spectrum associated with the vacancy-oxygen-carbon defect anneals at $T \sim 400^{\circ}$ C (Ref. 16). Hence the EPR data favors the vacancy-oxygen-carbon identification. Since this defect is positively charged (Ref. 16) it is unlikely that it would form complexes with lithium. Also, there is no evidence that lithium interacts with carbon in silicon. Hence it appears likely that lithium interacts with oxygen (Ref. 10) and vacancies (Ref. 17) to alter the structure of this defect.

Summary of Defect Interactions With Lithium

From the preceding it is suggested that lithium interacts with oxygen, single vacancies and divacancies to alter the structures of the deep level defects seen in the present boron doped cells. The question as to which one of these interactions is most effective in contributing to the increased radiation resistance of the counterdoped cells is open to speculation. However, we note that of the three deep level defects affected by lithium in boron doped silicon, the boron-oxygen complex is the only one whose production rate increases as cell resistivity and radiation resistance decrease (Ref. 11). This and the high minority carrier capture cross section of the $E_c - 0.27$ defect in the boron doped cell suggest that the lithium-oxygen interaction is most effective in contributing to the increased radiation resistance observed in the present lithium counterdoped cells.

CONCLUSIONS

As a result of this work, it is concluded that:

1. Lithium counterdoping results in significant increases in radiation resistance when compared to the 1 ohm-cm boron doped control cells.

2. Performance of irradiated counterdoped cells can be improved by annealing at 100° C.

3. The defect at $E_v + 0.43$ eV in the counterdoped cells is dominant in controlling the annealing behavior of the counterdoped cells.

4. The increased radiation resistance of the counterdoped cells is primarily due to the interaction of lithium with oxygen, single vacancies and divacancies. It is suggested that the lithium-oxygen interaction is the most effective in contributing to the increased radiation resistance.

APPENDIX

PREIRRADIATION I_{sc} AND V_{oc}

I_{sc}

Prior to irradiation, for all but cell Y-6, counterdoping tends to increase short circuit current. Insight into this behavior can be obtained from the spectral responses shown in Fig. 8. From the figure it is apparent that the emitter contribution to I_{sc} increases while the base contribution decreases as a result of counterdoping. Although only two counterdoped cells are shown, the behavior, shown in the figure, is observed for all of the counterdoped cells with cell Y-6 having the lowest long wavelength component. For all but this latter cell, the increased emitter component tends to dominate over the current loss experienced in the base. Reduction in the base component can be explained by noting that the field set up by the lithium gradient opposes and therefore tends to reduce the light induced current in the base. The low value of I_{sc} for cell Y-6 can be explained if one assumes that the counterfield set up by lithium in the base of this cell is sufficiently greater than that of the other counterdoped cells. However, the gradients of Table I do not correlate with this observation. Explanation for this apparent anomaly can be obtained if one assumes that the lithium gradient in cell Y-6 is zero over a sufficient distance extending from the rear of the cell such that the magnitude of the field in this cell, near the junction, is greatest and sufficiently strong for the base component to predominate over the emitter.

With regard to the emitter contribution to I_{sc}, we were unable to determine lithium concentrations in this region of the cell. It is noted however, that the lithium was introduced by ion-implantation into both the front and rear of the cell. Hence, the possibility exists that there is more lithium at the front of the cell than at the junction. In this case, the assumed lithium gradient in the emitter would generate a field which would aid the light induced current flow and thus tend to increase the emitter contribution to I_{sc}.

V_{oc}

The open circuit voltage can be expressed by the relation

$$V_{oc} = (AkT/q) \ln (I_{sc}/Io) \qquad (A1)$$

where $A = 1$ for injection-diffusion as the mechanism for dark current generation and $A = 2$ if a space charge region recombination mechanism prevails. Io is the reverse saturation current. From Eq. A-1, it is the increase in this latter component which causes the observed reductions in V_{oc}. Figure 9 is a plot of Io calculated for the present cells with $A = 1$ and illustrates the range of values for the observed reverse saturation currents. The values shown are typical of currents due to the injection-diffusion component. This component consists of electrons from the n-side, injected under forward bias, over the potential barrier at the junction, into the base region where they diffuse and drift, eventually recombining either in the bulk or at the surface. A similar current exists in the emitter due to holes injected from the p-side to the n-side. We note that the field due to lithium in the base is such that it tends to increase the dark current component from the base. On the other hand, the assumed field direction, due to lithium, in the emitter is such that it tends to decrease the emitter component of dark current. Hence, it is concluded that the reduced values obtained for V_{oc} are due primarily to an increase in the base component of Io, the increase in base component being great enough to more than compensate for a decrease in the emitter component of the reverse saturation current.

REFERENCES

1. JPL-TR-32-1514 (NASA CR-116793) 1971. Effects of lithium doping on the behavior of silicon and silicon solar cells, Berman, P A.

2. JPL-Pub-82-69 1982. Solar cell radiation handbook, Tada H Y et al.

3. Mandelkorn J et al 1962, Fabrication and characteristics of phosphorus-diffused silicon solar cells, J Electrochem. Soc. 109, 313-318.

4. Herman A M et al 1980, Radiation damage in lithium-counterdoped n/p silicon solar cells, Proc. 14th Photovoltaic Specialists Conf, San Diego 7-10 January 1980, 840-846.

5. Lang D V 1974, Deep level transient spectroscopy: a new method to characterize traps in semiconductors, J Appl. Phys. 45, 3023-3032.

6. The cells used in this study were fabricated by Mark Spitzer at the Spire Corp.

7. Godlewski M P et al 1973, The drift field model applied to the lithium-containing silicon solar cell, Conf. Record 10th Photovoltaic Specialists Conf, Palo Alto 13-15 November 1973, 378-383.

8. Faith T J 1972, Voltage and power relationships in lithium-containing solar cells, Conf. Record 9th Photovoltaic Specialists Conf, Silver Spring 2-4 May 1972, 292-295.

9. Young R C et al 1969, Interactions of Li and O with radiation produced defects in Si, J Appl. Phys. 40, 271-278.

10. Chrenko R M et al 1965, Vibrational spectra of lithium-oxygen & lithium-boron complexes in silicon, Phys. Rev. 138A(6), A1775-A1784.

11. Mooney P M et al 1977, Defect energy levels in boron-doped silicon irradiated with 1-MeV electrons, Phys. Rev. 15B(8), 3836-3843.

12. DeAngelis H M & Drevinsky P J, Influence of oxygen on defect production in electron-irradiated, boron-doped silicon, Proc Space Photovoltaic Research and Technology Conf, Cleveland 18-20 October 1983.

13. Watkins C D & Corbett J W 1965, Defects in irradiated silicon:electron paramagnetic resonance of the divacancy, Phys. Rev. 138A(2), 543-555.

14. Kimerling L C 1977, Defect states in electron bombarded silicon: capacitance transient analysis, Radiation Effects in Semiconductors, London, Institute of Physics, 221-230.

15. Brower K L 1974, EPR of a Jahn-Teller distorted ⟨111⟩ carbon Interstitialcy in irradiated silicon, Phys. Rev. 9B(6), 2607-2516.

16. Lee Y H et al 1977, EPR of a carbon-oxygen-divacancy complex in irradiated silicon, Phys. Status Solidi A 41, 637-647.

17. Naber J A et al 1971, Lithium-an impurity of interest in radiation effects of silicon, Radiat. Eff. 8, 239-244.

18. Watkins G D and Brower K L 1976, EPR of the isolated interstitial carbon atom in silicon, Phys. Rev. Let, 36(22), 1329-1332.

TABLE I. - PRE-IRRADIATION CELL CHARACTERISTICS

Cell	Resistivity[a]	Li gradient, cm^{-4}	I_{sc}, mA	V_{oc}, mV	P_{max}, mW	FF, percent
Control	1	---------	97.1	595	44	76.1
Z-10	1.8	1.6×10^{17}	98.3	540	39.5	74.4
Y-11	1.4	5.2×10^{16}	100.4	494	33	66.5
Z-3	1.7	2.2×10^{17}	100.8	508	36.2	70.7
Y-6	1.5	2.6×10^{16}	96.2	541	39.8	76.4
Z-12	1.7	2.1×10^{17}	101.3	505	36.5	71.3
Y-7	1.4	1.2×10^{17}	100.1	555	41.6	74.9

[a]Except for control: measured at back contact after introduction of lithium. All cells 2 by 2 cm, 250 μm thick: no AR coating.

TABLE II. - ENERGY LEVELS AND CAPTURE CROSS SECTIONS

		1 ohm-cm boron doped				1.8 ohm-cm counterdoped			
Energy level, eV		$E_V + 0.23$	$E_V + 0.26$	$E_V + 0.33$	$E_C - 0.27$	$E_V + 0.28$	$E_V + 0.43$	$E_V + 0.52$	$E_C - 0.46$
Capture cross section, cm^2	σp	3×10^{-16}	4×10^{-17}	2×10^{-16}		8.5×10^{-16}	2×10^{-13}	1×10^{-14}	
	σN				3×10^{-13}				9.3×10^{-18}

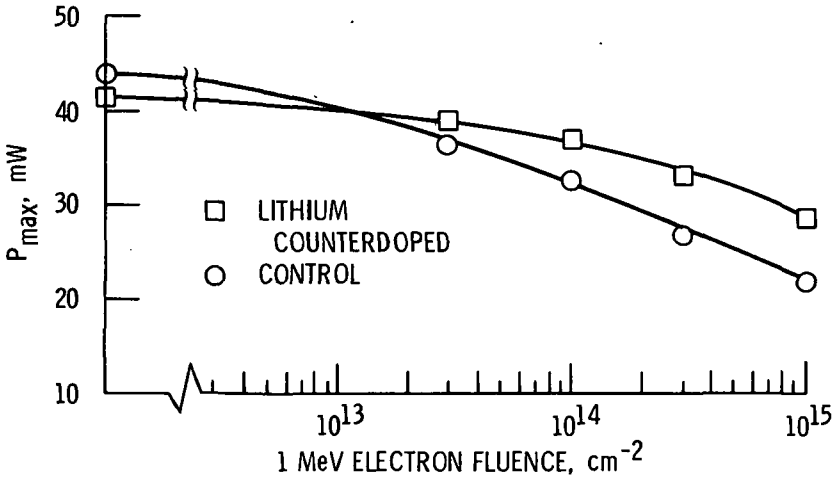

Figure 1. - P_{max} versus 1 MeV electron fluence.

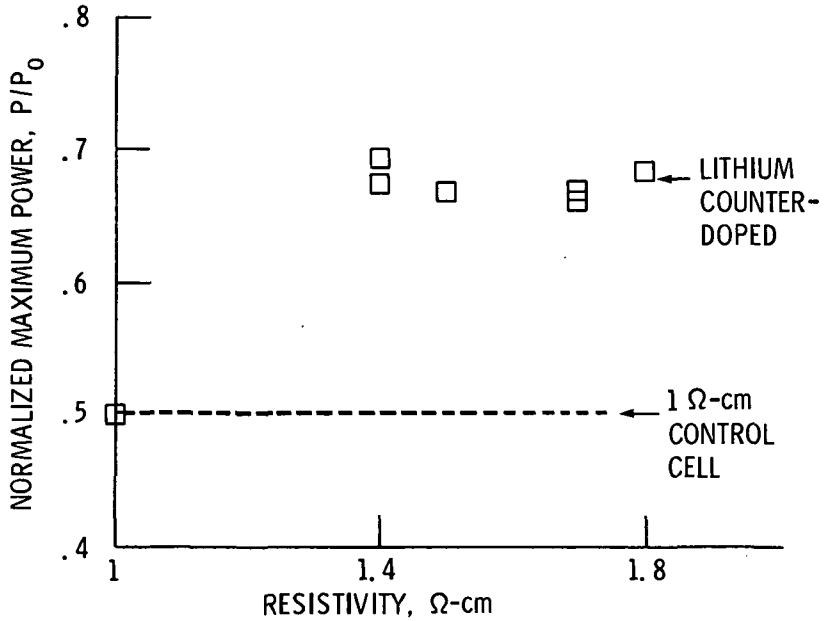

Figure 2. - Normalized maximum power for lithium counterdoped and boron doped control cells; $\Phi = 10^{15}/cm^2$.

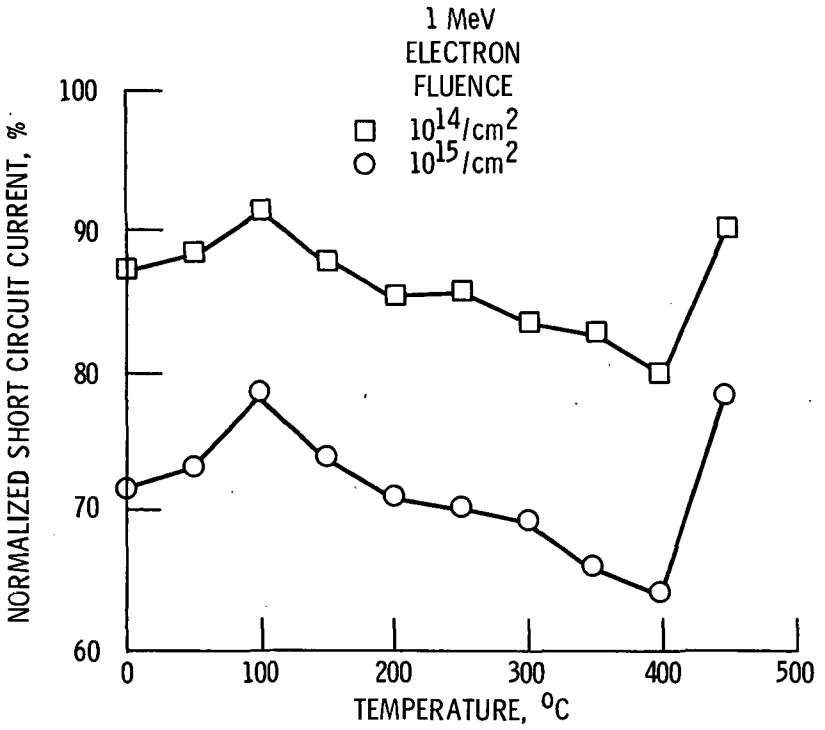

Figure 3. - Isochronal anneal of lithium counterdoped silicon cells.

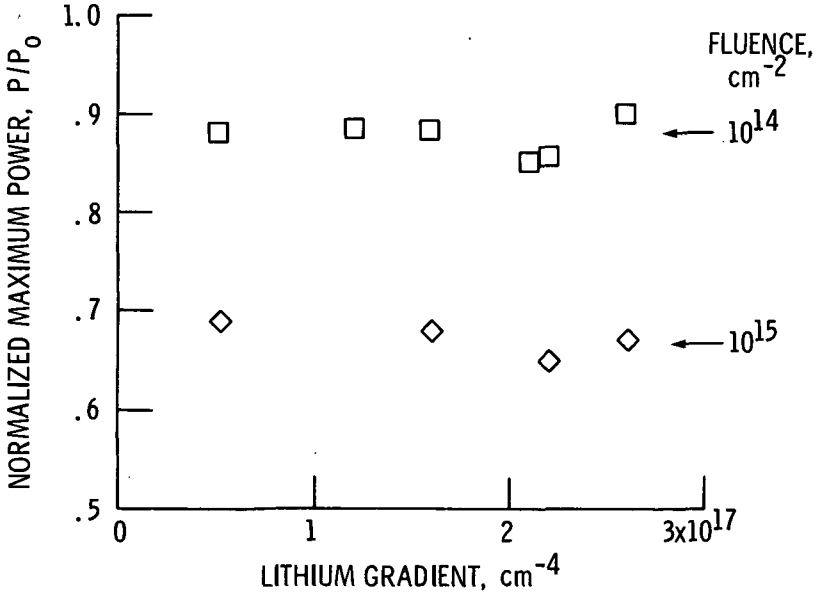

Figure 4. - Lithium gradient versus normalized maximum power-lithium counterdoped cells.

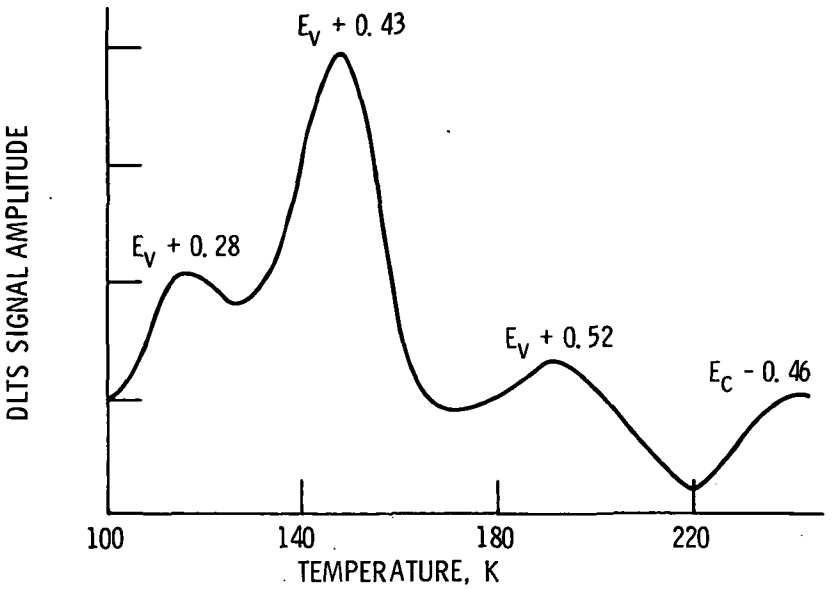

Figure 5. - DLTS spectrum of lithium counterdoped silicon cells after 1 MeV electron irradiation.

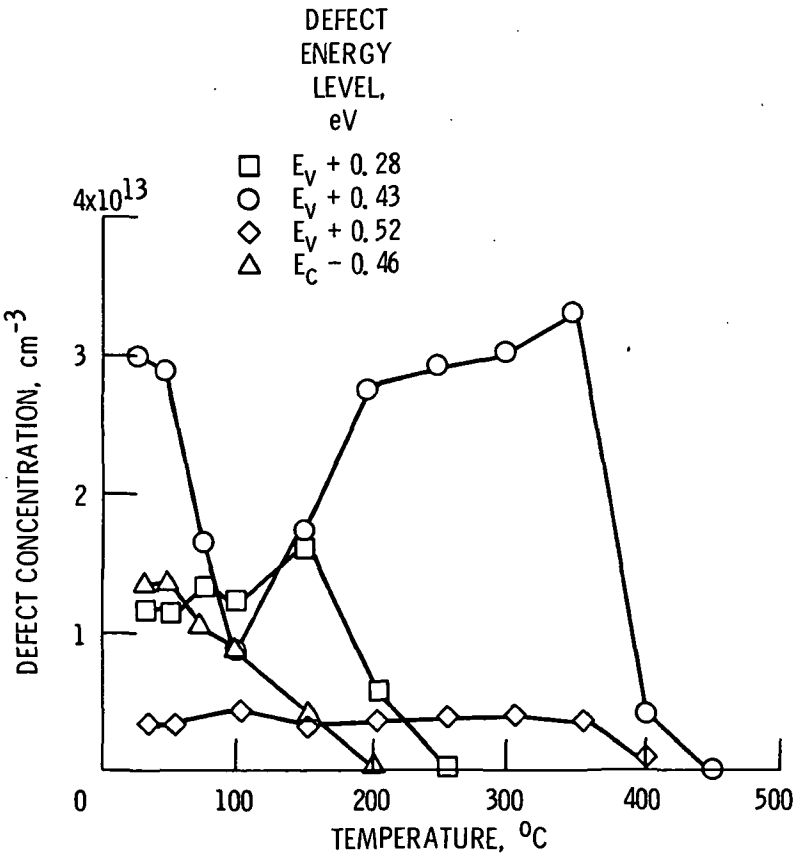

Figure 6. - Isochronal anneal of defects in lithium counterdoped silicon solar cells using DLTS.

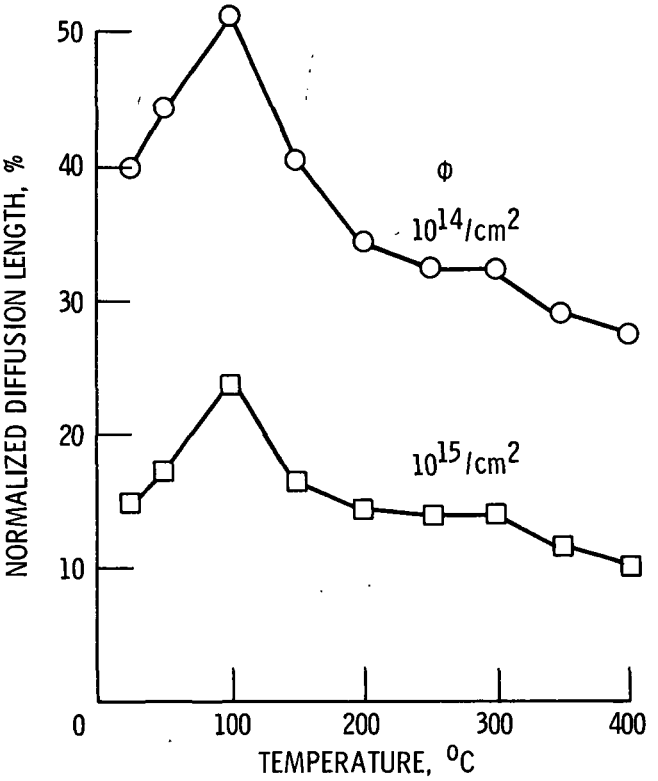

Figure 7. - Normalized diffusion length versus annealing temperature - lithium counter-doped cells.

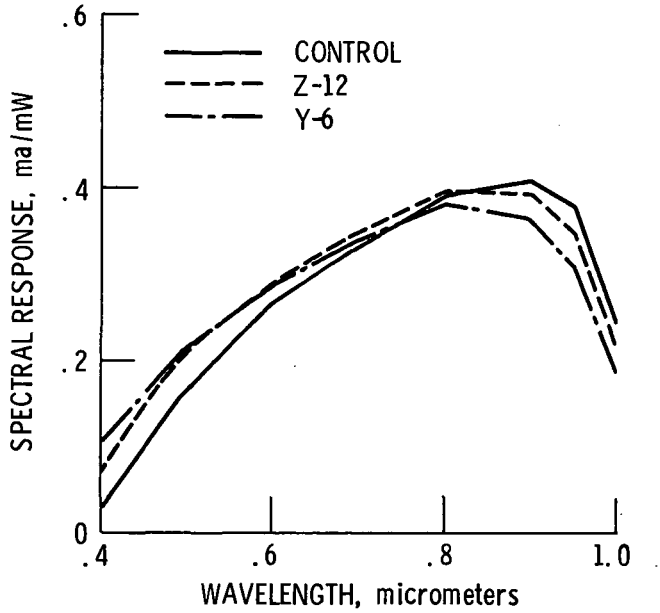

Figure 8. - Spectral response of control and several counterdoped cells.

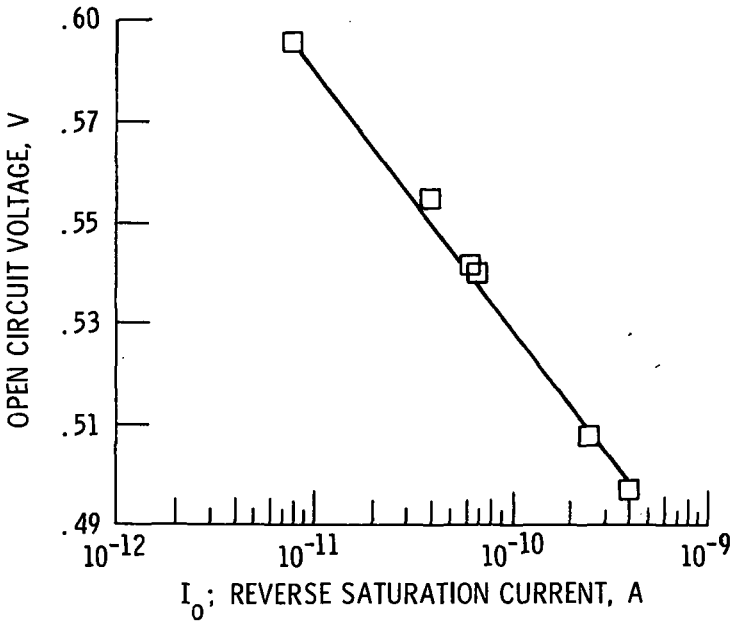

Figure 9. - Reverse saturation currents computed for the present cells.

1. Report No.	2. Government Accession No.	3. Recipient's Catalog No.
NASA TM-83755		

4. Title and Subtitle	5. Report Date
The Effects of Lithium Counterdoping on Radiation Damage and Annealing in n^+p Silicon Solar Cells	6. Performing Organization Code 506-55-42

7. Author(s)	8. Performing Organization Report No.
I. Weinberg, H. W. Brandhorst, Jr., S. Mehta, and C. K. Swartz	E-2243
	10. Work Unit No.

9. Performing Organization Name and Address	11. Contract or Grant No.
National Aeronautics and Space Administration Lewis Research Center Cleveland, Ohio 44135	13. Type of Report and Period Covered Technical Memorandum

12. Sponsoring Agency Name and Address	14. Sponsoring Agency Code
National Aeronautics and Space Administration Washington, D.C. 20546	

15. Supplementary Notes

Prepared for the Fourth European Symposium on Photovoltaic Generators in Space, Cannes, France, September 18-20, 1984. I. Weinberg, H. W. Brandhorst, Jr., and C. K. Swartz, Lewis Research Center; S. Mehta, Cleveland State University, Cleveland, Ohio and NASA intern.

16. Abstract

Boron-doped silicon n^+p solar cells were counterdoped with lithium by ion implantation and the resultant n^+p cells irradiated by 1 MeV electrons. Performance parameters were determined as a function of fluence and a Deep Level Transient Spectroscopy (DLTS) study was conducted in order to correlate defect behavior with cell performance. It was found that the lithium counterdoped cells exhibited significantly increased radiation resistance when compared to boron doped control cells. Isochronal annealing studies of cell performance indicate that significant annealing occurs at 100° C. Isochronal annealing of the deep level defects showed a correlation between a single defect at $E_V + 0.43$ eV and the annealing behavior of short circuit current in the counterdoped cells. It was concluded that the annealing behavior was controlled by dissociation and recombination of this defect. The DLTS studies also showed that counterdoping with lithium eliminated at least three deep level defects and resulted in three new defects. It was speculated that the increased radiation resistance of the counterdoped cells is due primarily to the interaction of lithium with oxygen, single vacancies and divacancies and that the lithium-oxygen interaction is the most effective in contributing to the increased radiation resistance.

17. Key Words (Suggested by Author(s))	18. Distribution Statement
Radiation damage; Lithium counterdoped silicon solar cells; Defects	Unclassified - unlimited STAR Category 33

19. Security Classif. (of this report)	20. Security Classif. (of this page)	21. No. of pages	22. Price*
Unclassified	Unclassified		

*For sale by the National Technical Information Service, Springfield, Virginia 22161

National Aeronautics and
Space Administration

Washington, D.C.
20546

Official Business
Penalty for Private Use, $300

SPECIAL FOURTH CLASS MAIL
BOOK

Postage and Fees Paid
National Aeronautics and
Space Administration
NASA-451

NASA

POSTMASTER: If Undeliverable (Section 158
Postal Manual) Do Not Return